Neuron, Vol. 34, 521–533, May 16, 2002, Copyright ©2002 by Cell Press

Neuronal α-Synucleinopathy with Severe Movement Disorder in Mice Expressing A53T Human α-Synuclein

Benoit I. Giasson,[1] John E. Duda,[1,2] Shawn M. Quinn,[1] Bin Zhang,[1] John Q. Trojanowski,[1] and Virginia M.-Y. Lee[1,3]
[1]Center for Neurodegenerative Disease Research
Department of Pathology and Laboratory Medicine
3600 Spruce Street
University of Pennsylvania School of Medicine
[2]Parkinson's Disease Research, Education and Clinical Center
Philadelphia Veterans Administration Hospital
3900 Woodland Avenue
Philadelphia, Pennsylvania 19104

Summary

α-Synucleinopathies are neurodegenerative disorders that range pathologically from the demise of select groups of nuclei to pervasive degeneration throughout the neuraxis. Although mounting evidence suggests that α-synuclein lesions lead to neurodegeneration, this remains controversial. To explore this issue, we generated transgenic mice expressing wild-type and A53T human α-synuclein in CNS neurons. Mice expressing mutant, but not wild-type, α-synuclein developed a severe and complex motor impairment leading to paralysis and death. These animals developed age-dependent intracytoplasmic neuronal α-synuclein inclusions paralleling disease onset, and the α-synuclein inclusions recapitulated features of human counterparts. Moreover, immunoelectron microscopy revealed that the α-synuclein inclusions contained 10–16 nm wide fibrils similar to human pathological inclusions. These mice demonstrate that A53T α-synuclein leads to the formation of toxic filamentous α-synuclein neuronal inclusions that cause neurodegeneration.

Introduction

α-Synuclein (α-syn) is a small (i.e., 140 amino acids) protein predominantly expressed in neurons and concentrated at synaptic terminals (George et al., 1995; Jakes et al., 1994). Although the function(s) of α-syn is ill defined, evidence suggests potential roles in neural plasticity and regulation of synaptic vesicle pools (George et al., 1995; Murphy et al., 2000). Foremost interest in α-syn surfaced with the recognition that it is the major component of pathological intracellular proteinaceous inclusions characteristic of specific neurological disorders, including Parkinson's disease (PD), Lewy body (LB) variant of Alzheimer's disease (LBVAD), dementia with LB (DLB), neurodegeneration with brain iron accumulation type-1 (NBIA-1) (formerly known as Hallervorden-Spatz disease), and multiple system atrophy (MSA) (Baba et al., 1998; Duda et al., 2000; Galvin et al., 2000; Spillantini et al., 1997, 1998; Tu et al., 1998). This recognition of α-syn pathology in a large number of neurodegenerative diseases is due to the remarkable discovery that in dominantly inherited α-syn substitutions, A53T was found in at least 12 families with familial PD albeit they likely share a common ancestor (Polymeropoulos et al., 1997; Golbe, 1999; Spira et al., 2001).

Neuronal α-syn inclusions occur as classical LBs, i.e., round, filamentous aggregates comprised of a core and halo that are detected by conventional histological stains, especially in dopaminergic neurons of the substantia nigra pars compacta (SNpc) of PD patients (Forno, 1996). However, the vast majority of neuronal α-syn lesions, including cortical LBs, other neuronal inclusions, neuroaxonal spheroids, and dystrophic neurites (termed Lewy neurites), were not fully appreciated until recently, and they are reliably detected by immunocytochemistry with antibodies to α-syn (Baba et al., 1998; Spillantini et al., 1997, 1998). Indeed, using newly developed antibodies to different modified forms of α-syn, the neuropathology of α-synucleinopathies are being redefined (Duda et al., 2002a). For example, in the Contursi kindred with the A53T α-syn mutation, extensive α-syn neuritic pathology was detected throughout the brain, including the limbic system, striatum, and locus coeruleus. In fact, neuritic pathology is much more abundant than perikaryal inclusions, and the substantia nigra was not the most severely affected brain nuclei (Duda et al., 2002b; Spira et al., 2001). α-Syn inclusions also accumulate in oligodendrocytes of patients afflicted by MSA, but these lesions, termed glial cytoplasmic inclusions, are largely restricted to this disorder (Duda et al., 2000; Tu et al., 1998). Finally, in situ and in vitro biochemical assessments indicate that all α-syn inclusions consist of bundles of 10–25 nm filaments comprised of polymerized α-syn (Baba et al., 1998; Giasson et al., 1999; Spillantini et al., 1998; Tu et al., 1998).

PD is the most widely recognized α-synucleinopathy since it is the most common movement disorder, with a prevalence of ~1% at 65 years of age and increasing to 4%–5% by the age of 85 (de Rijk et al., 1997). It is characterized clinically by bradykinesia, resting tremor, rigidity, postural instability, and periods of freezing (Simuni and Hurtig, 2000). In PD, neuronal α-syn pathology is concentrated in brainstem nuclei, including the SNpc and locus coeruleus (Forno, 1996). On the other hand, DLB and LBVAD are characterized by dementia, parkinsonism, hallucinations, and the presence of widespread and abundant neuronal α-syn inclusions and neurites (McKeith et al., 1996). Although α-syn pathologies are the defining neuropathological hallmarks of α-synucleinopathies, their role in disease pathogenesis and how they contribute to impaired cellular function, as well as brain degeneration, remains unresolved. This is further confounded by the fact that a threonine at amino acid residue 53 is the normal α-syn sequence found in rodent (Hsu et al., 1998). Thus, despite the demonstration that A53T α-syn has increased propensity to polymerize in vitro (Giasson et al., 1999), these results suggest, but do not unequivocally prove, that aggregates formed by α-syn fibrils are pathogenic. The observation that α-syn polymerization in vitro is concentration dependent (Gi-

[3]Correspondence: vmylee@mail.med.upenn.edu

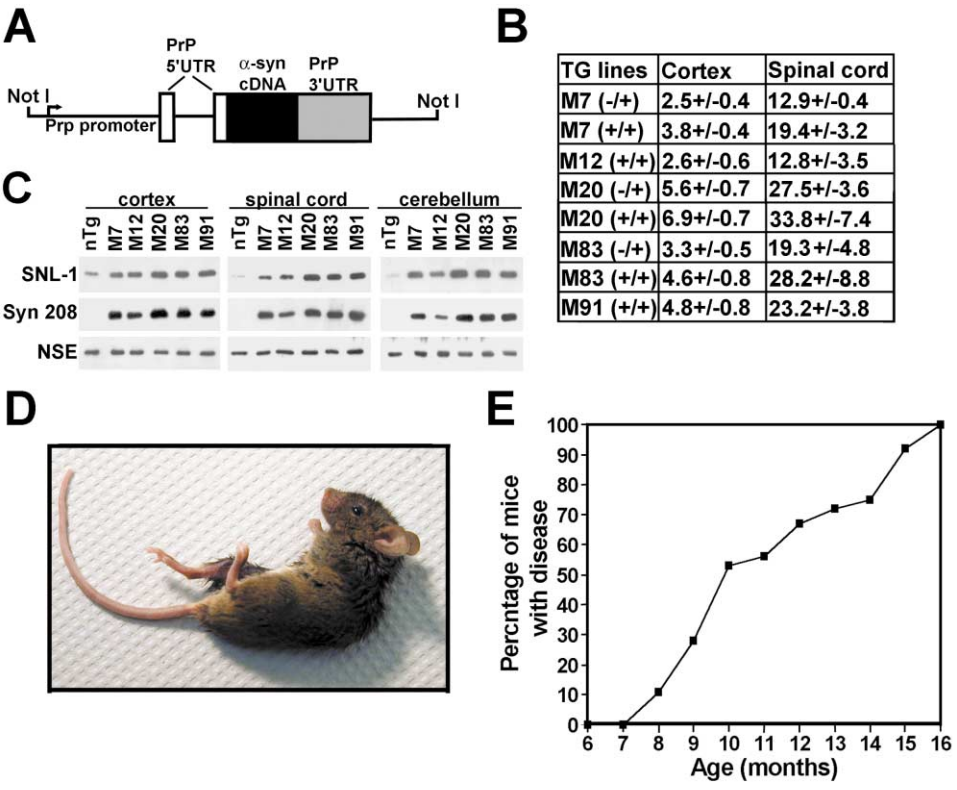

TG lines	Cortex	Spinal cord
M7 (-/+)	2.5+/-0.4	12.9+/-0.4
M7 (+/+)	3.8+/-0.4	19.4+/-3.2
M12 (+/+)	2.6+/-0.6	12.8+/-3.5
M20 (-/+)	5.6+/-0.7	27.5+/-3.6
M20 (+/+)	6.9+/-0.7	33.8+/-7.4
M83 (-/+)	3.3+/-0.5	19.3+/-4.8
M83 (+/+)	4.6+/-0.8	28.2+/-8.8
M91 (+/+)	4.8+/-0.8	23.2+/-3.8

Figure 1. Tg Lines Expressing Human α-Syn Driven by the Murine PrP Promoter and Motor Impairment Due to A53T Pathological Mutant

(A) Schematic of the transgene. Wild-type and A53T human α-syn cDNAs were cloned into the XhoI site of MoPrP.Xho mammalian expression vector. The resulting constructs are comprised of the murine PrP promoter, the 5′UTR of the PrP gene containing an intron, the human α-syn cDNA, and the 3′UTR of the PrP gene (not drawn to scale).

(B) Quantitative Western blot analysis of α-Syn overexpression in 3-month-old hemizygous (−/+) or homozygous (+/+) Tg mice. Lines M7, M12, and M20 express wild-type human α-syn, while lines M83 and M91 express A53T mutant human α-syn. Equal amounts of protein were loaded on SDS-PAGE gels, and the intensity of the α-syn immunoblot band was quantified with ^{125}I-Protein A. The signal was also further standardized to the levels of NSE (n = 3).

(C) Representative Western blots of nitrocellulose membranes probed with SNL-1 (specific for mouse and human α-syn), Syn 208 (specific for human α-syn), or anti-NSE antibodies and developed with ECL. The samples were obtained from nTg or homozygous mice from each Tg line.

(D) Photograph of a 9-month-old homozygous M83 Tg mouse displaying quadriparesis, arched back, and impaired axial rotation to upright posture.

(E) Onset of motor phenotype in M83 homozygous mice (n = 40).

asson et al., 1999; Wood et al., 1999) raises the possibly that an increased abundance of α-syn may contribute to the formation of pathological inclusions. To test this hypothesis and assess the consequence of expressing the A53T α-syn in the neurons of intact animals, transgenic (Tg) murine lines overexpressing equivalent levels of wild-type or A53T human α-syn were generated. Mice expressing the mutant A53T protein developed a lethal movement disorder linked to accumulations of pathological α-syn lesions that resembled authentic human neuronal inclusions.

Results

Generation of Tg Mice that Overexpress Wild-Type and A53T Human α-Syn

To generate Tg mice that express wild-type and mutant A53T human α-syn, the respective cDNAs were cloned into the MoPrP.Xho expression plasmid (Figure 1A), which drives high expression of the transgene in most CNS neurons (Borchelt et al., 1996). Tg lines expressing wild-type (lines M7, M12, and M20) or mutant A53T (lines M83 and M91) human α-syn were bred to homozygosity (see Experimental Procedures). The levels of α-syn expression in homozygous Tg mice were determined by quantitative Western blot (Figure 1B), and representative Western blots are depicted in Figure 1C. Neuronal-specific enolase (NSE) levels were measured and used as a control for equivalent loading of protein extracts. The anti-α-syn specific antibody SNL-1, which reacts equally with murine and human α-syn (Giasson et al., 2000b), was used to detect and quantify total α-syn. Syn 208, which is specific for human α-syn (Giasson et al., 2000b), was used to detect transgene expression exclusively. The relative levels of overexpression of α-syn, compared to endogenous levels, were much higher in the spinal cord than in the cortex (Figure 1B), but this is due to the lower amounts of endogenous α-syn in the spinal cord than in the cerebral cortex (see Figure 1C). The absolute level of α-syn expression within the cortex,

spinal cord, and cerebellum of each Tg line was similar (Figure 1C). For example, the ratio of total α-syn in the cortex versus cerebellum and spinal cord was 1.0 ± 0.4:1.4 ± 0.4:1.0 ± 0.3 for Tg line M7 and 1.0 ± 0.2:1.7 ± 0.4:1.4 ± 0.1 for Tg line M83. Homozygous mice from lines M7, M83, and M91 expressed similar levels of α-syn, while expression in line M12 was slightly lower in all three regions analyzed biochemically (Figures 1B and 1C). Homozygous mice from line M20 expressed the highest levels of α-syn than any other Tg mouse lines (Figure 1B). The level of overexpression in hemizygous Tg mice was more than half the level of homozygotes. For example, the level of overexpression in the cortex of M20 hemizygotes is 5.6 ± 0.7, compared to 6.9 ± 0.7 for M20 homozygotes, while it is 3.3 ± 0.5 for M83 hemizygotes, compared to 4.6 ± 0.8 for M83 homozygotes.

Homozygous Tg mice expressing wild-type or A53T mutant human α-syn remained healthy without any overt phenotype up to the age of 7 months. At this point, mice did not have muscle weakness, as determined by their ability to stand on a slanted surface. Furthermore, up to this age, homozygous mice expressing either wild-type (line M7) or A53T (line M83) human α-syn did not exhibit any impaired performance on the rotarod task: nTg = 306.2 ± 11.0 (n = 12), M7 homozygous = 316.4 ± 12.0 (n = 12), and M83 homozygous = 349.3 ± 17.3 (n = 8). By 8 months of age, a few homozygous mice expressing A53T α-syn began to develop a dramatic motor phenotype. The initial changes included neglect of grooming, weight loss, and reduced ambulation. These changes were followed by severe movement impairment with resistance to passive movement and partial paralysis of limbs, accompanied by periods (several seconds) of freezing of a hindlimb. Tremulous motion was observed in some recumbent animals, possibly related to attempted muscular activity. Paralysis of the extremities usually began at a hindleg, but within a few days, all four limbs became affected. At this time, mice also were unable to right themselves when placed on their sides, and they developed hunched backs (Figure 1D) (see supplemental video clips online at http://www.neuron.org/cgi/content/full/34/4/521/DC1). The animals eventually were unable to stand up and support their own body weight. Affected mice became unable to feed themselves in a standard cage, but their lifespan could be prolonged for a few days by bottom feeding. Within 10–21 days of the first signs of disease, animals were sacrificed to prevent suffering. Notably, by contrast to many other mouse models of human disease (Cote et al., 1993; Ishihara et al., 1999; Lee et al., 1994), normal and affected α-syn Tg mice did not show retraction of their hind limbs when held inverted by the tail.

To date, all homozygous Tg animals from lines M83 (Figure 1E) and M91 (data not shown) have developed the phenotype described above within 16 months of age. Many hemizygous animals from line M83 also developed the same phenotype, but the age of onset was between 22 and 28 months of age. So far, none of the hemizygous mice from line M91 up to the age of 28 months have been affected. No neurological phenotype was observed in any of the hemizygous or homozygous Tg mice expressing wild-type human α-syn (lines M7 and M12) up to 28 months of age. Similarly, hemizygous and homozygous mice from line M20 as old as 24 months and 14 months, respectively, have not displayed any neurological phenotype.

Histological Characterization of α-Syn Pathology

Immunostaining for α-syn in homozygous mice of lines M7 and M12, up to the age of 26 months, revealed the normal neuropil staining pattern (data not shown) expected for this protein (Giasson et al., 2001; Jakes et al., 1994). Similar results were obtained for 24-month-old hemizygous and 14-month-old homozygous mice of line M20. The same immunostaining pattern also was observed in all homozygous Tg mice expressing the A53T mutant protein until the age of 6 months (data not shown). Furthermore, no differences were detected in the localization of human or mouse α-syn using species-specific antibodies (data not shown). However, in homozygous A53T mutant α-syn animals ranging between 8 to 16 months of age, α-syn inclusions in the somatodendritic compartment and dystrophic neurites became abundant and widely distributed throughout the neuraxis (Figures 2, 3, 4, and 5). A high density of inclusions was observed in the spinal cord (Figures 2A–2D and 3F), throughout the brainstem (Figures 2E–2J, 3B–3E, and 4A), the deep cerebellar nuclei (Figure 2K), deep cerebellar white matter, and some regions of the thalamus, such as the medioventral, ventromedial, and paracentral nuclei (summarized in Figure 3). A gradient of neuritic pathology was found in the striatum with the densest accumulation in the dorsolateral part (Figures 2L and 3A), and sparse pathology was found in motor cortex (Figure 3). Other regions of the cerebral cortex, the olfactory bulb, and the hippocampus were devoid of α-syn pathology. Certain cell populations were completely spared, including the Purkinje cells and granular cells in the cerebellum and tyrosine hydroxylase (TH)-positive neurons of the substantia nigra. In homozygous M83 and M91 A53T mutant α-syn Tg mice, the earliest age that pathology has been observed is 7 months of age, with scant α-syn aggregates detected. The same profile of α-syn inclusions was only detected in hemizygous Tg mice of line M83 between 22 and 28 months of age, when animals developed the motor phenotype described above.

While many perikaryal α-syn lesions filled the entire somatodendritic compartment, some were more distinct structures reminiscent of cortical LBs in humans. These LB-like inclusions were abundant in the raphe nuclei (Figure 2E) and the pons (Figures 2F and 2G) and less abundant in locus coeruleus (data not shown). Some of the inclusions in the locus coeruleus were in TH-positive neurons (Figures 4C–4E). α-Syn inclusions in neuronal processes appeared as dystrophic neurites (Figures 2C, 2F, and 2H), reminiscent of LNs in human diseases (Figures 5A and 5B), as well as larger neuroaxonal spheroids (Figure 2D). Occasional α-syn ovoids were also detected in the sciatic nerve (data not shown).

α-Syn inclusions were robustly detected with several antibodies (i.e., Syn 303, Syn 505, Syn 506, and Syn 514) raised to oxidized α-syn that preferentially recognize pathological α-syn in human brain tissue from patients with synucleinopathies (Duda et al., 2002a). The labeling of inclusions with a panel of conventional α-syn antibod-

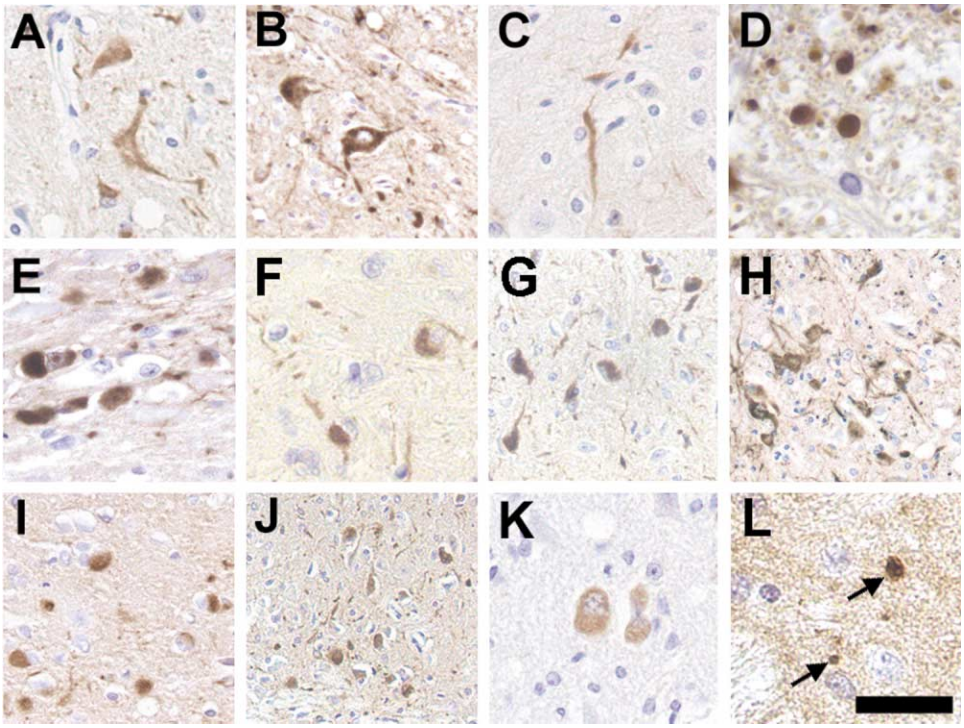

Figure 2. Representative α-Syn Pathology in Neuronal Cell Bodies and Processes

Immunocytochemistry was performed as described in Experimental Procedures. In the spinal cord, pathology included diffuse perikaryal inclusions in the ventral horn (A and B), and dystrophic neurites and spheroid-like inclusions in the gray matter (C) or ventral white matter (D), detected with SNL-4 (A, C, and D) or Syn 303 (B). In addition, LB-like inclusions were found in the raphe nucleus (E) and pons (F and G) and were stained with Syn 303 (E) and Syn 505 (F and G). Abundant α-syn pathology was also seen in neuronal perikarya and processes in the pontine reticular nuclei (H and I), locus coeruleus (J), and deep cerebellar nuclei (K) stained with Syn 303 (I), Syn 506 (H), or Syn 505 (J and K). Occasional dystrophic neurites were seen in the striatum (L) stained with Syn 505 (L). Stained tissue sections of homozygous M83 mice are depicted in (A)–(E), (G) and (H), and (J)–(L), hemizygous M83 mice in (I), and homozygous M91 mice in (F). The age of mice in the micrographs depicted: 12 months old in (A), (C), (D), and (G)–(H); 14 months old in (B), (E), (J), and (L); 16 months old in (F); 22 months old in (I); and 9 months old in (K).

Bar = 40 μm in (A), (C), (E)–(H), and (K); 80 μm in (B) and (J); 20 μm in (D) and (L); 50 μm in (I).

ies was variable: robust staining with SNL-4, moderate staining with Syn 202 and LB509, and weak staining with Syn 211, Syn 102, and Syn 204. These α-syn lesions, especially those in neuronal processes, are strikingly reminiscent of inclusions found in human synucleinopathies, including patients with the A53T substitution (see Figures 5A and 5B), and they do not contain β-syn or γ-syn, since they were not detected by anti-β-syn (Syn 207) or anti-γ-syn (γ-1) antibodies. Likewise, there was also a paucity of staining with phosphorylation-dependent anti-neurofilament (NF) antibodies (e.g., RMO55 and RMO24), but in contrast, another phosphorylation-dependent anti-NF antibody (RMO32), which was found previously to label many LBs in human PD and DLB cases (Schmidt et al., 1991), labeled some of the α-syn inclusions (Figure 5C). Approximately 10%–25% of α-syn inclusions also demonstrated ubiquitin immunoreactivity (Figures 5D and 5E).

Consistent with neuronal injury in affected Tg mice expressing A53T α-syn, significant astrocytic gliosis was observed with glial fibrillary acidic protein (GFAP) staining (Figure 5F). However, quantitative analysis of motor spinal neurons did not reveal a significant loss of these cells, even in mice displaying severe motor impairment: motor impaired M83 Tg mouse = 16.5 ± 0.5 neurons/section and non-Tg mouse = 16.7 ± 0.8 neurons/section. This finding is consistent with the short time interval between appearance of pathological changes and presentation of phenotype changes. In common with authentic human pathological lesions (Giasson et al., 2000a), α-syn inclusions in mice contained 3-nitro-tyrosine (Figures 5G and 5H), were impregnated with silver (Figures 5I–5K), and stained with thioflavin S (Figures 5L and 5M).

Accumulation of Insoluble and Aggregated α-Syn in A53T α-Syn Tg Mice

The spinal cord, cerebellum, and cortex of non-Tg (nTg) and Tg mice expressing wild-type (M7) and A53T (M83) human α-syn were sequentially extracted with buffers with increasing strength of protein solubilization. Western blotting was used in conjunction with antibodies specific for mouse and human α-syn (SNL-1) or only human α-syn (LB509), as well as an anti-α-syn antibody that preferentially recognizes pathological α-syn (Syn 303) to detect α-syn in these fractions. In nTg mice, the majority of α-syn was recovered in the high-salt (HS) and HS/Triton X-100 (T) fractions, but a small amount could also be observed in the RIPA fraction (Figure 6). In M7 mice, the distribution profile was similar to nTg

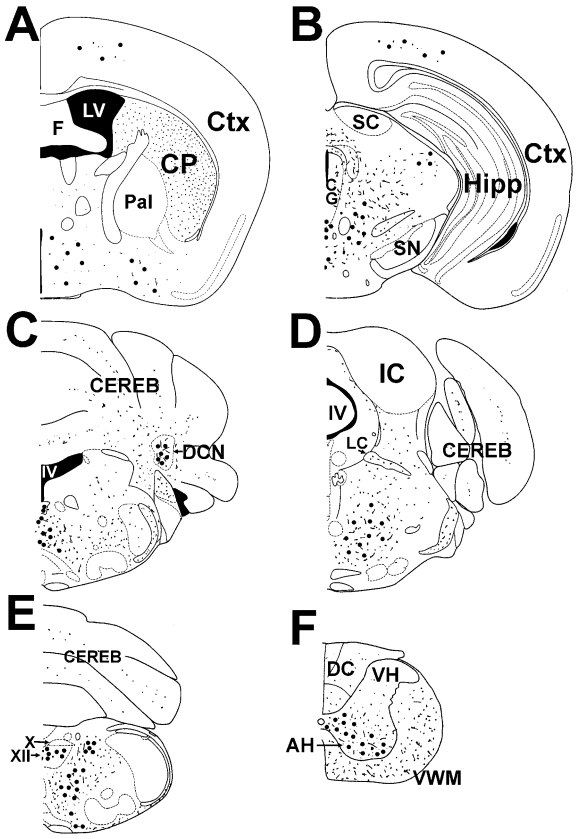

Figure 3. Schematic of the Distribution of α-Syn Pathology in A53T α-Syn Mice

Diagrammatic summary of α-syn pathology shown as coronal sections of the mouse neuroaxis at the levels of the pallidum (A), superior colliculi (B), deep cerebellar nuclei (C), inferior colliculi (D), hypoglossal nucleus (E), and cervical spinal cord (F). Large dots represent perikaryal inclusions, while curvilinear markings and small dots correspond to neuritic dystrophy. Abbreviations: AH, anterior horn; CEREB, cerebellum; CG, central gray matter; CP, caudoputamen (striatum); Ctx, neocortex; DC, dorsal columns; DCN, deep cerebellar nuclei; F, fornix; HIPP, hippocampus; IC, inferior colliculus; IV, fourth ventricle; LC, locus coeruleus; LV, lateral ventricle; Pal, pallidum; SC, superior colliculus; SN, substantia nigra; VH, ventral horn; VWM, ventral white matter; X, dorsal motor nucleus of vagus; and XII, hypoglossal nucleus.

mice, but there was an increase in α-syn in the RIPA fraction of all three anatomical regions analyzed (Figure 6), and there was also a small amount in the SDS-soluble fraction of the spinal cord (Figure 6A) and cerebellum (Figure 6D). It is possible that this α-syn in the SDS-soluble fractions may correspond to protein aggregates that are not abundant enough to be seen by light microscopy. There was a significant accumulation of RIPA-insoluble (i.e., SDS- or FA-soluble) α-syn in the spinal cord (Figure 6A) and cerebellum (Figure 6D) of M83 mice, and a lesser amount was also present in the cortex (Figure 6G) (for quantitation, see supplemental data online at http://www.neuron.org/cgi/content/full/34/4/521/DC1). RIPA-insoluble α-syn in M83 mice was comprised of human A53T mutant α-syn (Figures 6B, 6E, and 6H). Aggregated α-syn that did not enter the resolving gels was also detected in the HS- and SDS-soluble fractions of the spinal cord of M83 mice (Figures 6A–6C). Furthermore, protein bands that are likely cross-linked dimers and trimers of α-syn were detected in the SDS- and FA-soluble fractions of the spinal cord of M83 mice using antibody Syn 303 (Figure 6C).

Ultrastructural Analysis of Pathological Changes

Toluidine blue-stained semi-thin sections from the ventral root of nTg (Figure 7A), M7 Tg mice (Figure 7B), and M83 Tg mice (Figure 7C) revealed significant axonal degeneration and an increase in the endoneurial compartment in aged mice expressing A53T α-syn (Figure 7C). At the ultrastructural level, many degenerating axons associated with deteriorating myelin could be observed (Figure 7D). However, the initial phase of the degenerative process appeared to involve axons, since many severely degenerating axons were still surrounded by relatively intact myelin sheaths (Figures 7E and 7F). It appears that following axonal degeneration, myelin sheath loosens and unravels (Figure 7G), eventually forming multilamellar myelin debris (Figures 7H and 7I). Occasionally, these structures were surrounded by macrophages that appeared to remove debris (data not shown). Longitudinal (Figure 7J) and axial views (Figure 7K) of axons filled with vacuoles suggested local blockage of axonal transport. Similarly, disarrayed bundles of NFs were also observed (Figure 7L). Eosin/hematoxylin staining of the gastrocnemius muscle revealed sparse neurogenic muscle atrophy in A53T mice with impaired movement (data not shown), consistent with a rapidly progressive axonal neuropathy.

Immunoelectron microscopy of the spinal cord of A53T mice demonstrated the intense and specific labeling of α-syn inclusions in axons (Figure 8A). Detachment and retraction of the axolemma could be observed in proximity of α-syn inclusions (Figure 8B), indicative of axonal degeneration. Aggregation of α-syn in the periphery of the axolemma was also noted in some axons (Figure 8C), a profile seen in human carriers of the A53T mutation (see Discussion). Higher magnification of immunolabeled α-syn lesions demonstrated that they were predominantly comprised of ~10–16 nm fibrils (Figures 8D–8F). The specific labeling directly on the fibrils suggests that these polymers are comprised of α-syn. Perikaryal α-syn inclusions were also comprised of similar immunolabeled filaments (Figures 9A and 9B). Furthermore, α-syn-labeled fibrils are ultrastructurally distinct from NFs. A side by side comparison of filaments immunolabeled with α-syn antibodies and a longitudinal view of NFs from the same A53T α-syn Tg mouse demonstrate this difference (Figures 9C and 9D). α-Syn immunolabeled fibrils are much shorter and irregular (Figure 9C), and they do not have the side arms characteristic of NFs (Figure 9D) (Lee and Cleveland, 1996; Julien and Mushynski, 1998). To further confirm that inclusions were comprised of filamentous α-syn, we isolated α-syn fibrils biochemically, using a method previously developed for pathological human brain (Spillantini et al., 1998). Filaments were clearly immunolabeled with antibodies to α-syn in preparations from the cerebellum (Figure 9E), spinal cord (Figure 9F), and pons (Figures 9G and 9H) from A53T α-syn Tg mice. Furthermore, isolated α-syn filaments were not labeled with antibodies to NFs in double-labeling experiments (data not shown).

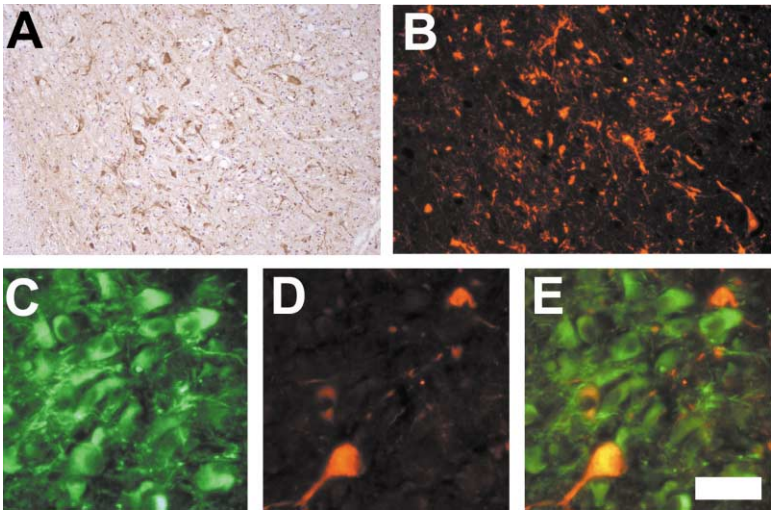

Figure 4. Characterization of α-Syn Inclusions in A53T α-Syn Mice

Low-power light microscopy of α-syn inclusions in the pons of a 12-month-old homozygous M83 mouse immunolabeled with antibody Syn 505 (A). Immunofluorescence microscopy of spinal cord stained with Syn 303 in a 12-month-old homozygous M83 mouse reveals abundant inclusions in neuronal cell bodies and processes (B). A section of the locus coeruleus from a 12-month-old homozygous M83 mouse were double-labeled with anti-TH ([C], green) and Syn 505 ([D], red) antibodies. Syn 505 staining reveals that some of TH-expressing cells in the locus coeruleus also contain α-syn aggregates (composite image in [E]).

Scale = 140 μm in (A); 80 μm in (B); 40 μm in (C)–(E).

Discussion

The dramatic behavioral phenotype associated with the formation of α-syn inclusions in mice expressing A53T human α-syn represent an excellent model of α-synucleinopathies. This model has a robust phenotype leading to the demise of the animals and neuronal dysfunction that coincides with the formation of α-syn aggregates. These finding represent compelling evidence for the detrimental role of α-syn inclusion formation, a position that is still controversial. Furthermore, the α-syn inclusions in these mice recapitulate all aspects of the typical characteristics of human inclusions, and similar to humans, these mice display significant α-syn aggregation in both

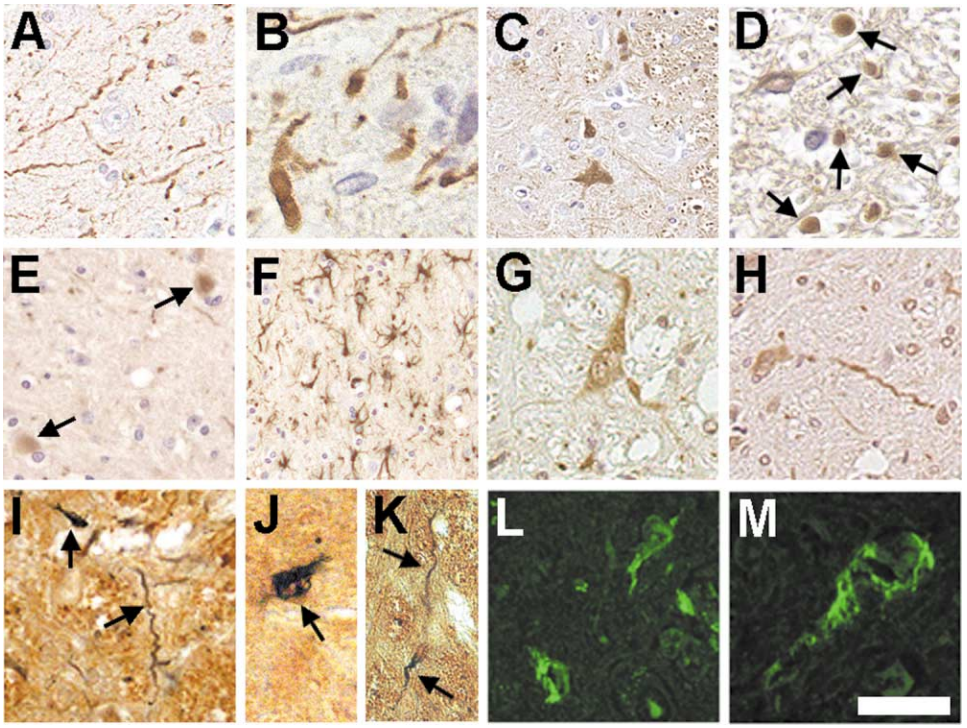

Figure 5. Properties of Inclusion in A53T α-Syn Mice

For comparison of the inclusions in the mice and human-expressing A53T α-syn, we have included micrographs demonstrating abundant LNs and neuroaxonal spheroids detected with Syn 303 in the entorhinal cortex of a patient of the Contursi kindred harboring the A53T α-syn substitution (A and B). In mice expressing A53T human α-syn, some inclusions (exemplified here in spinal cord) were also labeled with anti-NF antibody RMO32 (C) and with anti-ubiquitin antibodies (D and E). Also depicted in the spinal cord, GFAP immunoreactivity revealed astrocytic gliosis (F). The presence of 3-nitro-tyrosine in α-syn inclusions in the pons was detected with nSyn 823 (G and H). α-Syn pathology was visualized by silver (I–K) and thioflavin S staining (L and M). Arrows were placed to highlight pathological inclusions. Stained tissue sections of 12-month-old homozygous M83 mice are depicted in (C)–(M).

Bar = 40 μm in (A), (E), (G), (H), (K), and (L); 80 μm in (F); 20 nm in (B), (D), (J), and (M); 50 μm in (C); and 33 μm in (I).

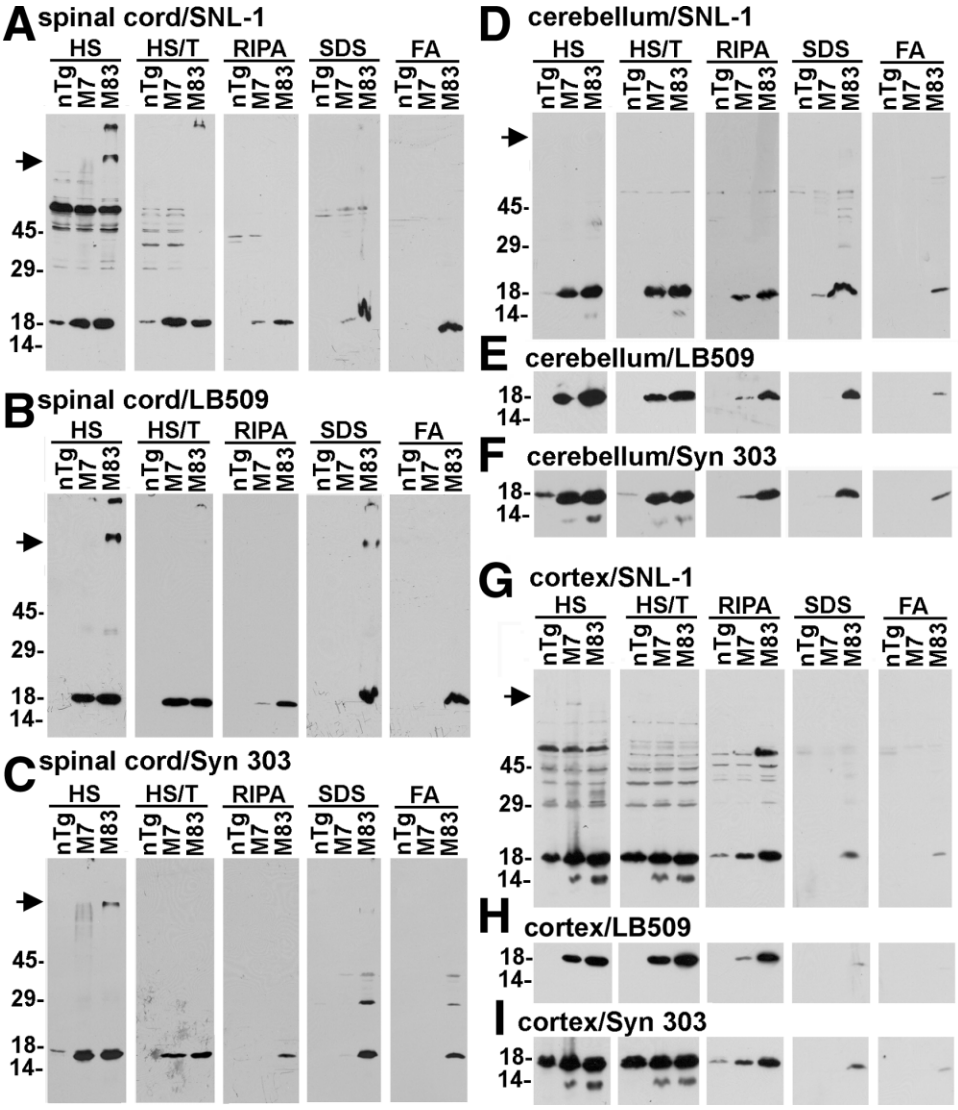

Figure 6. Accumulation of Insoluble and Aggregated α-Syn in Mice Expressing A53T Mutant α-Syn

Samples of spinal cord (A–C), cerebellum (D–F), and neocortex (G–I) from 9-month-old nTg, homozygous M7 Tg (M7), and homozygous M83 Tg (M83) mice were sequentially extracted, as described in Experimental Procedures. HS-, HS/T-, RIPA-, SDS-, and formic acid (FA)-soluble fractions were analyzed by Western blotting using antibody SNL-1 (α-syn specific), antibody LB509 (human α-syn specific), and antibody Syn 303 (preferentially recognizes pathological α-syn). The positions of molecular mass markers are depicted on the left. The arrow indicates the resolving and stacking gel interface.

neuronal cell bodies and processes. Moreover, the specificity of the pathological changes in mice expressing A53T human α-syn, in contrast to the lack thereof in mice expressing the wild-type protein, provides further credence to the notion that this amino acid substitution leads to neurodegeneration by promoting the formation of filamentous inclusions.

The A53T α-syn mutation in humans is generally described as resulting in clinical PD with a notably early age of onset (~45 years of age) (Golbe et al., 1996; Spira et al., 2001). However, the clinical presentation includes several features (such as dementia, prominent myoclonus, and urinary incontinence) that are not characteristic of PD, especially considering the young age of the individuals (Golbe et al., 1996; Spira et al., 2001). Consistent with these findings, examination of the distribution of α-syn pathology in autopsy tissue revealed that it is significantly more widespread throughout the neuraxis than in PD (Spira et al., 2001; Duda et al. 2002b). As in idiopathic PD, LBs were observed in midbrain nuclei; however, diffusely distributed neuritic pathology was the prominent finding. Similarly, aggregation of α-syn in neuronal processes was a major feature of Tg mice from lines M83 and M91 (see Figures 2, 3, 4A, and 4B). Also, the profile of aggregated α-syn at the periphery of axolemma in Tg mice (Figure 8C) is akin to inclusions observed in a patient with the A53T mutation (Duda et al., 2002b).

Several other Tg mouse models expressing wild-type and mutant α-syn have been described recently, but these models neither revealed the differences between wild-type and mutant α-syn nor did they fully recapitu-

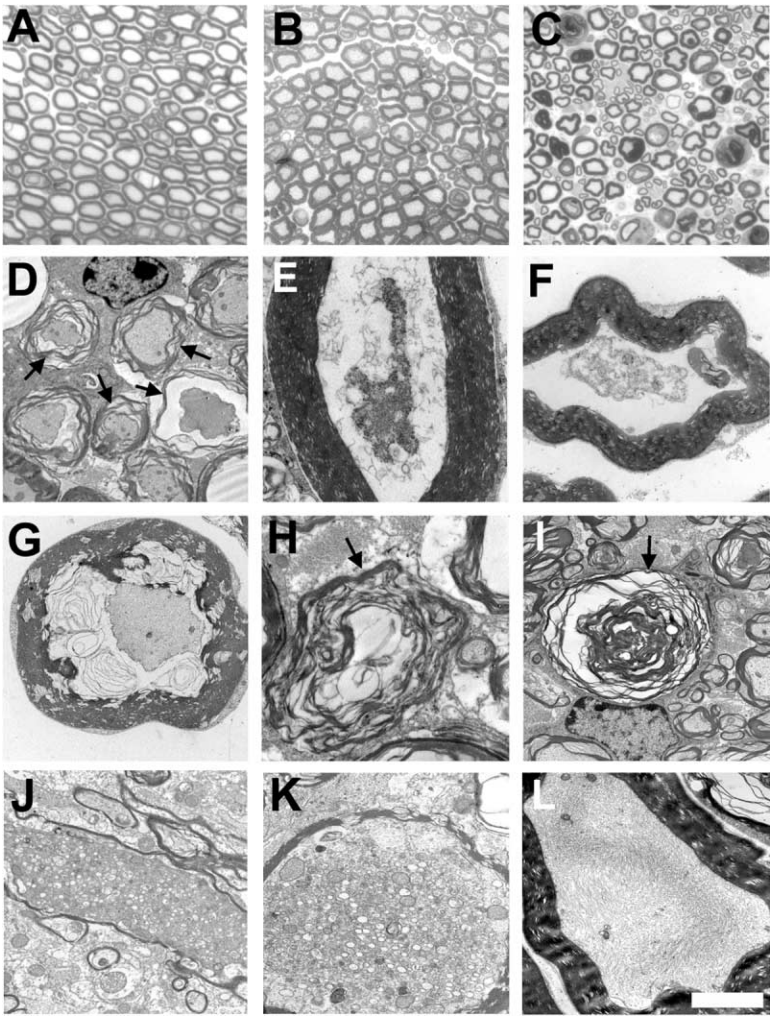

Figure 7. Wallerian Degeneration in Ventral Roots of A53T α-Syn Mice

Representative semi-thin sections of L5 ventral roots from 12-month-old nTg (A), homozygous M7 Tg (B), and homozygous M83 Tg (C) mice. Note the extensive axonal degeneration and increased endoneurial space in M83 mice. Ultrastructural analysis of ventral roots by transmission electron microscopy reveals abundant axonal degeneration characterized by axonal atrophy and demyelination (D). Axonal degeneration without disruption of the contiguous myelin sheath (E and F). Axonal atrophy accompanied by degeneration of contiguous myelin resulting in loosening of myelin wraps (G) and the formation of multilamellar bodies (H and I). Aberrant axonal swellings containing accumulations of vacuoles, vesicles, and mitochondria (J and K) and bundles of disarrayed NFs (L) in the ventral root of homozygous M83 Tg mice. Bar = 30 μm in (A)–(C); 4 μm in (D); 1 μm in (E) and (K); 2 μm in (F), (G), and (L); 1.5 μm in (H) and (J); and 3 μm in (I).

late the characteristics of human α-syn pathology (Kahle et al., 2000; van der Putten et al., 2000). The comparison of these different models is complicated by the use of different promoters, which have varied expression in specific neuronal populations. This caveat notwithstanding, other groups have used the human platelet-derived growth factor-β (PDGF-β) and the murine Thy-1 promoter to express human α-syn in mice. In the study utilizing the PDGF-β promoter, expression of wild-type protein resulted in the formation of amorphous, nonfilamentous α-syn aggregates associated with impairment of motor function and reduction in striatal TH terminals (Masliah et al., 2000). A subset of α-syn inclusions also contained ubiquitin, which is characteristic of authentic human inclusions (Love and Nicoll, 1992). However, unexpectedly (and at odds with reported human synucleinopathies), a significant portion of these inclusions were located in the nucleus.

Expression of wild-type and A53T or A30P mutant α-syn in Tg mice driven by the Thy-1 promoter results in the appearance of perikaryal and neuritic accumulations but without notable differences between wild-type and mutant proteins (Kahle et al., 2000; van der Putten et al., 2000). In one study, mice expressing wild-type or A53T mutant α-syn developed an early onset motor impairment (>3 weeks of age), as measured by rotating rod performance, and this phenotype was associated with axonal degeneration in the spinal root and muscle denervation (van der Putten et al., 2000). A subset of α-syn inclusions in these mice were argyrophillic and immunoreactive for ubiquitin, but they lacked the filamentous characteristic of authentic human α-syn inclusions. On the other hand, expression of wild-type or mutant human α-syn in *Drosophila* results in the formation of filamentous α-syn inclusions concomitant with the demise of dorsomedial dopaminergic neurons and impairment of locomotor function (Feany and Bender, 2000).

Our Tg mouse model has many similarities with human neuronal α-synucleinopathies (especially familial PD) due to the A53T α-syn mutation. Foremost, PrP-driven expression of human A53T α-syn results in a mid-to-late onset neurodegenerative disorder that coincides with the accumulation of filamentous α-syn cytoplasmic inclusions throughout the neuraxis, similar to patients with the A53T mutation. No α-syn pathology was detected in young animals (<6 months) expressing A53T human α-syn, and these animals did not present an overt neurological impairment. The onset of this disease is heralded by the appearance of sparse pathology without

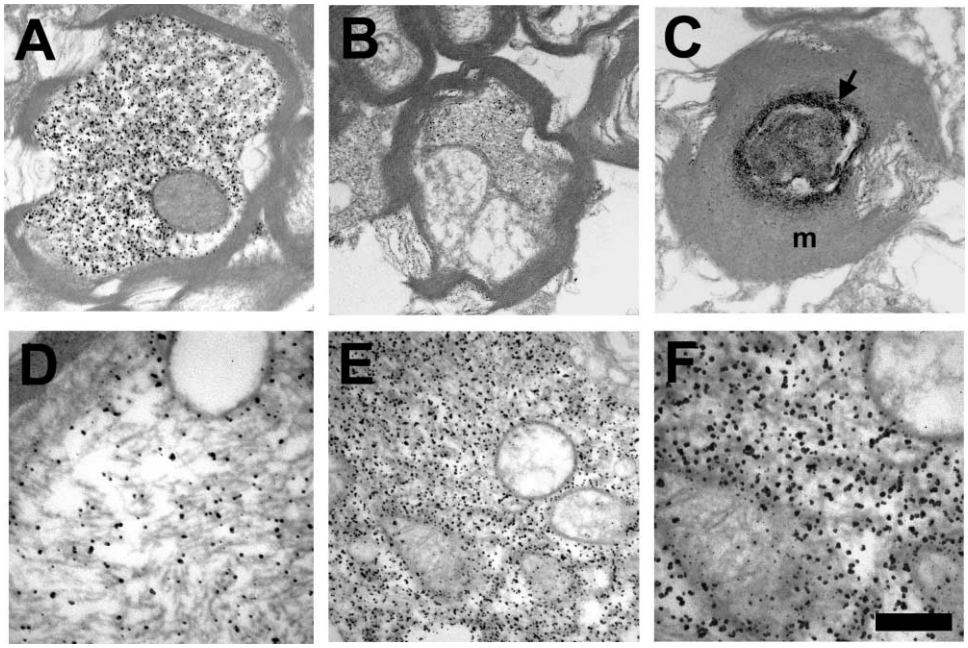

Figure 8. Immunoelectron Microscopy of α-Syn Inclusion in the Spinal Cord of M83 Tg Mice

(A) Immunolabeling of axonal α-syn aggregates with antibody Syn 303 demonstrates the specific labeling of a filamentous component.
(B) α-Syn accumulation is seen in an atrophied axon where the axolemma is detached from the myelin.
(C) Intense accumulation of α-syn also can occur at the periphery of the axolemma, as indicated by the arrow. "m" refers to the myelin sheath.
(D–F) Higher magnification of α-syn inclusions shows the labeling of ~10-16 nm wide fibrils.
Bar = 1.3 μm in (A) and (C); 1.7 μm in (B); 400 nm in (D); 600 nm in (E); and 300 nm in (F).

clinical manifestations similar to humans (Forno, 1996). The precise mechanism to account for the selective vulnerability of neurons affected in these mice remains unclear. However, the presence of α-syn pathology in motor neurons of the ventral horn and axons in the ventral root may contribute to motor impairment. Yet, the complex changes exhibited by mice expressing A53T human α-syn suggest dysfunction in other neuronal systems. Furthermore, the lack of clasping behavior, characteristic of other mouse models involving the demise

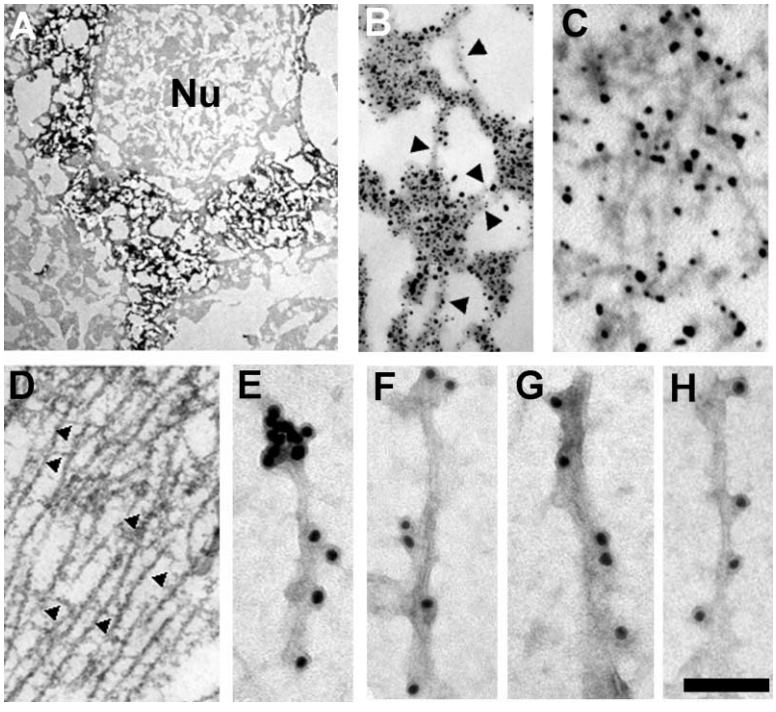

Figure 9. Inclusions in A53T α-Syn Tg Mice Are Comprised of Filamentous α-Syn

Immunoelectron microscopy of perikaryal inclusions in the deep cerebellar nuclei (A) of an 11-month-old homozygous M83 Tg mouse (Nu = nucleus). Higher magnification of the latter inclusion depicting immunolabeled filaments (B). Immunoelectron microscopy of a filamentous α-syn inclusion in the spinal cord of a 10-month-old homozygous M83 Tg mouse (C) and a micrograph depicting a longitudinal view of neurofilaments in the same animal (D). Note that the presence of side arms protruding from NFs are highlighted by arrow heads. Isolated α-syn filaments extracted form the cerebellum (E), spinal cord (F), and pons (G and H) of a 9-month-old homozygous M83 Tg mouse are labeled with antibodies Syn 303 (E–G) or LB509 (H). The dark particles are 10 nm colloidal gold conjugated to the anti-mouse antibody (see Experimental Procedures).
Bar = 4.9 μm in (A); 250 nm in (B); 190 nm in (C) and (D); 50 nm in (E), (F), and (H); and 55 nm in (G).

of motor neurons (Cote et al., 1993; Ishihara et al., 1999; Lee et al., 1994) suggests a different mechanism. The rapid and catastrophic presentation of the phenotype indicates either the synchronized formation of pathological lesions or the accumulation of neuronal injury that eventually surpasses a threshold for behavioral manifestations. In striking contrast to Tg mice expressing A53T α-syn, mice expressing wild-type human α-syn did not develop any form of aberrant α-syn accumulations or neurological defects, although it remains a possibility that older M20 mice may eventually be affected.

The location of pathological lesions in A53T mice does not completely correspond with human disorders, but it shares many similarities. Pathology was very abundant in the brain stem and in several nuclei affected in PD and DLB, such as the locus coeruleus and the raphe nucleus. Interestingly, the presence of striatal pathology coincides with human diseases (Shoji et al., 2000; Duda, et al., 2002a). Furthermore, the abundance of neuritic pathology is consistent with these disorders, and the formation of large axonal inclusions is reminiscent of human α-syn neuroaxonal spheroids, which are characteristic of NBIA-1. An obvious difference is the paucity of pathology in TH-expressing neurons of the substantia nigra. In mice, it does not appear that these neurons display the same selective vulnerability as in humans. A recent report using the TH promoter to express wild-type and mutant α-syn selectively in these neurons did not result in the formation of inclusions (Matsuoka et al., 2001). It is not clear why these neurons would have different cross-species properties, but the lack of neuromelanin formation in mice could be a determinant. Furthermore, this population of neurons may be protected from the formation of inclusions induced by Tg expression due to intrinsic protective mechanisms necessary to compensate for their normal heightened exposure to oxidative damage.

The immunological, histological, biochemical, and ultrastructural properties of inclusions in mice carrying human A53T α-syn closely resemble authentic human pathological inclusions. (1) α-Syn inclusions in these Tg mice share the characteristic immunological properties of authentic human lesions. They are strongly labeled with antibodies that preferentially mark human pathological inclusions (i.e., Syn 303, Syn 505, Syn 506, and Syn 514). (2) A subset of inclusions are selectively labeled with a phosphorylation-dependent anti-NFM antibody (RMO32), which is exceptional at labeling most LBs (Schmidt et al., 1991), but not with other phosphorylation-dependent NF antibodies. (3) A proportion of inclusions are modified by ubiquitin or 3-nitro-tyrosine. 3-Nitro-tyrosine was only detected in a small number of inclusions, indicating that the modification is likely not required for the formation of inclusions in Tg mice. However, it is possible that other nitrative modifications, especially o-o′ dityrosine cross-linking that occurs in concert with nitration and could be involved in the stabilization of some aggregates. (4) The presence of detergent-insoluble, as well as high molecular-mass, α-syn aggregates that do not enter the SDS-PAGE resolving gel is also similar to the properties of α-syn inclusions in human diseases (Baba et al., 1998; Dickson et al., 1999; Duda et al., 2000; Galvin et al., 2000). The accumulation of these high molecular-mass species and apparent dimers/trimers in A53T mice suggest that α-syn may be cross-linked by covalent modifications that could involve oxidative modification. (5) A significant number of α-syn inclusions in A53T mice, like authentic α-syn inclusions in human neurodegenerative diseases, are detected by Gallyas silver staining and amyloid-binding dyes (such as thioflavin S). (6) Finally, just like α-syn filaments found in LBs and Lewy neurites in human synucleinopathies, α-syn filaments from A53T mice are comprised of ~10–16 nm fibrils that are directly and intensely labeled with antibodies to α-syn.

The most likely explanation for the neurotoxicity of the A53T α-syn mutation resides in altered biophysical properties, since this mutation increases the propensity of α-syn to polymerize into fibrils in vitro, when compared to wild-type α-syn (Giasson et al., 1999). The formation of α-syn fibrils eventually leads to the formation of toxic neuronal inclusions. The depletion of functional α-syn due to sequestration in inclusions is not a factor in the pathogenicity, since ablation of α-syn in mice by gene targeting shows only mild electrophysiological and behavioral changes, but not an overt phenotype (Abeliovich et al., 2000). Thus, α-syn inclusions likely act as physical obstacles impeding the physiological movement of organelles and smaller cytoplasmic metabolites. This notion is supported by the changes observed in the axons of A53T Tg mice that include axonal enlargements filled with vacuoles or disorganized NF networks. The ultrastructural changes observed are consistent with a primary neuronal degeneration with subsequent myelin injury.

It can be surmised that the A53T mutation is pathological due to an increased propensity to form filamentous inclusions. An additional pathogenic insult seems to be required to induce the formation of similar lesions from wild-type α-syn, since simple overexpression of wild-type α-syn within the timeframe of these experiments is insufficient. One possibility is suggested by a recent study demonstrating that the presence of extracellular β-amyloid deposits increases the abundance and promotes the fibrillization of α-syn aggregates in PDGF-β Tg mice (Masliah et al., 2001). Experimental cell culture models suggest that oxidation or nitrative damage can result in the formation of α-syn aggregates (Paxinou et al., 2001), and LB-like inclusions can be induced in rats treated with rotenone (an inhibitor of the mitochondrial complex I), presumably due to increased oxidative stress (Betarbet et al., 2000). The mechanism involved in the formation of inclusions from wild-type human α-syn is still unclear, but the evidence that filamentous α-syn inclusions can be the major determinant of a number of neurodegenerative disorders underscores the importance of elucidating these pathways. This premise is supported by the findings herein and several pathological studies correlating LB density with severity of dementia in patients (Hurtig et al., 2000; Mattila et al., 2000).

The PrP mice expressing wild-type human α-syn will be useful in establishing putative cellular insights that promote formation of intracytoplasmic lesions. Furthermore, the A53T mice may be valuable in screening for potential therapeutics that inhibit or reverse α-syn aggregate formation. It is uncertain if the formation of α-syn inclusions is reversible, but this concept has been dem-

onstrated in other Tg models of neurodegenerative disease associated with proteinaceous inclusions (Schenk et al., 1999; Yamamoto et al., 2000) leading to novel therapeutic strategies.

Experimental Procedures

Generation of α-Syn Tg Mice

Wild-type human α-syn cDNA (Jakes et al., 1994) and the same cDNA harboring the A53T mutation were cloned into the MoPrP.Xho expression vector (Borchelt et al., 1996) at the XhoI restriction site. The 14 kb NotI linear fragments containing the α-syn cDNA and the mouse prion protein (PrP) gene promoter, together with its 5′ untranslated region (UTR) containing an intron and its 3′ untranslated sequences (Figure 1A), were used as the transgene to create α-syn Tg mice on a C57Bl/C3H background. The Tg DNA was microinjected into C57Bl/C3H mouse eggs as a service provided by the Transgenic and Chimeric Mouse Facility of the University of Pennsylvania. Genomic DNA samples were isolated from mouse tails with the Puregene DNA isolation kit (Gentra Systems, Minneapolis, MN). Potential founders were identified by Southern blot analysis with a ^{32}P-labeled oligonucleotide-primed α-syn DNA probe. Stable Tg lines carrying the wild-type (lines M7, M12, and M20) or mutant A53T (lines M83 and M91) human α-syn constructs were established, and Tg and wild-type offspring were identified by Southern blot analysis of tail DNA. Homozygous Tg lineages were identified by quantitative Southern blot analysis and verified by backcrossing.

Rotarod Task

This task for locomotor function was conducted using a Rota-Rod treadmill Model 7650 (Ugo Basile, Comerio, Italy), set with accelerating revolution (4–40 revolutions per min) over a 5 min period. Mice were given three trails a day for 3 consecutive days.

Antibodies

SNL-1 and SNL-4 are rabbit antibodies raised to synthetic peptides corresponding to amino acids 2–12 and 104–119 in α-syn, respectively (Giasson et al., 2000b). Syn 211, Syn 204, Syn 208, and LB 509 are mouse monoclonal antibodies specific for human α-syn, while Syn 102 and Syn 202 are mouse monoclonal antibodies that bind to both α- and β-syn (Giasson et al., 2000b). Syn 207 is a β-syn-specific mouse monoclonal antibody (Giasson et al., 2000b), and γ-1 is a γ-syn-specific rabbit antibody (Giasson et al., 2001). Syn 303, Syn 505, Syn 506, and Syn 514 are mouse monoclonal antibodies raised to oxidized human α-synuclein, as previously described (Giasson et al., 2000a). Although these antibodies do not recognize a specific oxidation modification, they preferentially recognize pathological α-syn inclusions (Duda et al., 2002a; B.I.G., unpublished data). nSyn 823 is a nitration-specific antibody raised to nitrated α-syn (Giasson et al., 2000a). Murine monoclonal antibodies RMO32 and RMO55 are specific for phosphorylated NF midsize subunit (NFM), and RMO24 is specific for phosphorylated NF heavy subunit (NFH) (Schmidt et al., 1991). Antibody 17026 is tau-specific rabbit polyclonal antibody and PHF-1 is mouse monoclonal antibody-specific for a phosphorylation epitope in tau. Anti-NSE (Polysciences, Inc., Warrington, PA), anti-GFAP (DAKO, Glostrio, Denmark), and anti-TH (Pelfreeze, Rogers, AK) are rabbit polyclonal antibodies. Anti-ubiquitin (MAB1510) was purchased from Chemicon International, Inc. (Temecula, CA).

Gel Electrophoresis and Western Blotting

Mouse tissues were dissected and disrupted in 2% SDS, 50 mM Tris (pH 6.8) by sonication and heated to 100°C for 10 min. Protein concentrations were determined using the biocinchoninic acid (BCA) assay (Pierce, Rockford, IL). Western blot analysis was performed as previously described (Giasson et al., 1999). Quantitative Western blotting was performed using ^{125}I-labeled protein A (NEN) as secondary antibody. NSE was included as an internal standard to monitor loading errors. The membranes were dried and exposed to a PhosphorImager plate. The radioactive signal was quantified using ImageQuant software (Molecular Dynamics, Inc., Sunnyvale, CA).

Immunocytochemistry

Mice, anesthetized with an intraperitoneal overdose injection of xylazine and ketamine, were perfused with phosphate-buffered saline (PBS), followed by 70% ethanol/150 mM NaCl or PBS buffered formalin. Following surgical removal of brain and spinal cord, tissue was fixed for another 24 hr in the respective fixatives. Samples were dehydrated through a series of graded ethanol solutions to xylene at room temperature, infiltrated with paraffin at 60°C as described in Trojanowski et al. (1989), and cut into serial 6 μm sections. Immunocytochemistry was conducted as previously described (Duda et al., 2000).

Double-Labeling Immunofluorescence

Double-labeling immunofluorescence studies were performed by incubating sections with Syn 505 and anti-TH antibodies. Following extensive washes, sections were labeled using Alexa Fluor 488 (green) and 594 (red) conjugated secondary antibodies (Molecular Probes, Eugene, OR) and covered with Vectashield-DAPI mounting medium (Vector Laboratories, Burlingame, CA).

Spinal Cord Neuronal Counting

The L2–L3 spinal cord segments of Tg and nTg mice were formalin fixed and paraffin embedded. The entire spinal cord segments were cut in 12 μM thick sections, which were stained with cresyl violet. Motor neurons in Rexed's laminae IX of the L2 and L3 spinal levels were counted by two observers.

Sequential Biochemical Fractionation

Cortex, cerebellum, and spinal cord from 9-month-old mice were dissected, weighed, and homogenized in 3 ml/g of HS buffer (50 mM Tris [pH 7.5], 750 mM NaCl, 5 mM EDTA, and a cocktail of protease inhibitors). The samples were sedimented at 100,000 × g for 20 min. Pellets were reextracted with HS buffer, followed by two sequential extractions with 3 ml/g of HS buffer containing 1% Triton X-100 (HS/T fraction). The pellets were homogenized in 500 μl of HS buffer/1 M sucrose, and, after centrifugation, the floating myelin was discarded. The pellets were extracted with 2 ml/g of RIPA (50 mM Tris [pH 8.0], 150 mM NaCl, 5 mM EDTA, 1% NP40, 0.5% sodium deoxycholate, and 0.1% SDS) and sedimented at 100,000 × g for 20 min. Half of each pelleted sample was extracted with 1 ml/g SDS sample buffer (SDS fraction) by sonication and heated to 100°C for 10 min in or 70% formic acid (FA fraction) by sonication. FA was removed by lyophilization, and the dried material was resuspended in 1 ml/g of SDS-sample buffer by heating to 100°C for 10 min. 5 μl of each fraction was loaded on separate lanes of 12% polyacrylamide gels, and the distribution of α-syn was determined by Western blotting analysis.

Conventional and Immunoelectron Microscopy

For direct electron microscopy, mice were deeply anesthetized and sacrificed by intracardiac perfusion with 0.1 M cacodylate buffer (pH 7.4), followed by 4% paraformaldehyde/2% glutaraldehyde in 0.1 M cacodylate (pH 7.4). The L5 segments of the spinal cord and L5 ventral roots were removed and further fixed for 18 hr. Tissue was postfixed with 2% osmium tetraoxide for 1 hr, dehydrated with graded ethanol solutions, and embedded in Epon.

Mice prepared for pre-embedding immunoelectron microscopy were perfused with 0.1 M cacodylate buffer (pH 7.4), followed by 2% paraformaldehyde/0.5% glutarldehyde in 0.1 M cacodylate (pH 7.4). The tissue was further fixed for 12 hr, washed with PBS, cut into 50 μM sections, and reacted with 0.1% sodium borohydrate in PBS for 10 min. Following extensive blocking, sections were labeled with antibody Syn 303 and sequentially incubated with a biotinylated goat anti-mouse antibody and ABC reagents. Following the reaction with DAB, tissue sections were further developed with silver methenamine, as previously described (Rodriguez et al., 1984). Sections were postfixed with 1.5% glutaraldehyde and 1% osmium tetraoxide, and, following dehydration in graded ethanol, they were embedded in Epon.

Isolation of Dispersed α-Syn Filament

α-Syn filaments were extracted from the pons, cerebellum, or spinal cord of 9-month-old motor-impaired M83 mice using a method pre-

viously described for human tissue (Spillantini et al., 1998). Briefly, tissue was homogenized in 50 mM Tris (pH 7.4), 750 mM NaCl, 2 mM EGTA, and 10% sucrose. After centrifugation at 14,000 × g for 20 min, the supernatant was incubated with 1% sarcosyl for 30 min. The solution was centrifuged at 100,000 × g for 1 hr, and the resulting pellet was resuspended in 50 mM Tris (pH 7.4). Aliquots of the dispersed filaments were applied onto carbon-coated 300-mesh copper grids. Grids were blocked with 1% bovine serum albumin in PBS and filaments were immunolabeled with anti-α-syn antibodies, followed by a goat anti-mouse antibody secondary conjugated to 10 nm gold. Fibrils were visualized by negative staining with 1% uranyl acetate.

Acknowledgments

This work was funded by grants from the National Institutes of Health and by a Pioneer Award from the Alzheimer's Association. V.M.-Y.L. is the John H. Ware III professor in Alzheimer's disease research. B.I.G. is the recipient of a fellowship from the Canadian Institutes of Health Research. We are grateful to Drs. Douglas C. Miller and Lawrence I. Golbe for providing tissue from a patient of the Contursi kindred and Mr. Daniel Martinez and Mr. Charles Graves, Jr., for their expert technical assistance.

Received: November 2, 2001
Revised: March 7, 2002

References

Abeliovich, A., Schmitz, Y., Farinas, I., Choi-Lundberg, D., Ho, W.H., Castillo, P.E., Shinsky, N., Verdugo, J.M., Armanini, M., Ryan, A., et al. (2000). Mice lacking alpha-synuclein display functional deficits in the nigrostriatal dopamine system. Neuron *25*, 239–252.

Baba, M., Nakajo, S., Tu, P.H., Tomita, T., Nakaya, K., Lee, V.M.-Y., Trojanowski, J.Q., and Iwatsubo, T. (1998). Aggregation of α-synuclein in Lewy bodies of sporadic parkinson's disease and dementia with lewy bodies. Am. J. Pathol. *152*, 879–884.

Betarbet, R., Sherer, T.B., MacKenzie, G., Garcia-Osuna, M., Panov, A.V., and Greenamyre, J.T. (2000). Chronic systemic pesticide exposure reproduces features of Parkinson's disease. Nat. Neurosci. *3*, 1301–1306.

Borchelt, D.R., Davis, J., Fischer, M., Lee, M.K., Slunt, H.H., Ratovitsky, T., Regard, J., Copeland, N.G., Jenkins, N.A., Sisodia, S.S., and Price, D.L. (1996). A vector for expressing foreign genes in the brains and hearts of transgenic mice. Genet. Anal. *13*, 159–163.

Cote, F., Collard, J.F., and Julien, J.P. (1993). Progressive neuronopathy in transgenic mice expressing the human neurofilament heavy gene: a mouse model of amyotrophic lateral sclerosis. Cell *73*, 35–46.

de Rijk, M.C., Tzourio, C., Breteler, M.M., Dartigues, J.F., Amaducci, L., Lopez-Pousa, S., Manubens-Bertran, J.M., Alperovitch, A., and Rocca, W.A. (1997). Prevalence of parkinsonism and Parkinson's disease in Europe: the EUROPARKINSON collaborative study. J. Neurol. Neurosurg. Psychiatry *62*, 10–15.

Dickson, D.W., Liu, W., Hardy, J., Farrer, M., Mehta, N., Uitti, R., Mark, M., Zimmerman, T., Golbe, L., Sage, J., et al. (1999). Widespread alterations of α-synuclein in multiple system atrophy. Am. J. Pathol. *155*, 1241–1251.

Duda, J.E., Giasson, B.I., Gur, T.L., Montine, T.J., Robertson, D., Biaggioni, I., Hurtig, H.I., Stern, M.B., Gollomp, S.M., Grossman, M., et al. (2000). Immunohistochemical and biochemical studies demonstrate a distinct profile of α-synuclein permutations in multiple system atrophy. J. Neuropathol. Exp. Neurol. *59*, 830–841.

Duda, J.E., Giasson, B.I., Mabon, M.E., Lee, V.M.-Y., and Trojanowski, J.Q. (2002a). Novel antibodies to oxidized α-synuclein reveal abundant neuritic pathology in Lewy body diseases. Ann. Neurol., in press.

Duda, J.E., Giasson, B.I., Mabon, M., Miller, D.C., Golbe, L.I., Lee, V.M.-Y., and Trojanowski, J.Q. (2002b). Concurrence of α-synuclein and tau pathology in a Contursi kindred brain. Acta. Neuropathol., in press.

Feany, M.B., and Bender, W.W. (2000). A *Drosophila* model of Parkinson's disease. Nature *404*, 394–398.

Forno, L.S. (1996). Neuropathology of Parkinson's disease. J. Neuropathol. Exp. Neurol. *55*, 259–272.

Galvin, J.E., Giasson, B., Hurtig, H.I., Lee, V.M.-Y., and Trojanowski, J.Q. (2000). Neurodegeneration with brain iron accumulation, type 1 is characterized by α-, β- and γ-synuclein neuropathology. Am. J. Pathol. *157*, 361–368.

George, J.M., Jin, H., Woods, W.S., and Clayton, D.F. (1995). Characterization of a novel protein regulated during the critical period for song learning in the zebra finch. Neuron *15*, 361–372.

Giasson, B.I., Uryu, K., Trojanowski, J.Q., and Lee, V.M.-Y. (1999). Mutant and wild type human α-synucleins assemble into elongated filaments with distinct morphologies in vitro. J. Biol. Chem. *274*, 7619–7622.

Giasson, B.I., Duda, J.E., Murray, I.V., Chen, Q., Souza, J.M., Hurtig, H.I., Ischiropoulos, H., Trojanowski, J.Q., and Lee, V.M.-Y. (2000a). Oxidative damage linked to neurodegeneration by selective α-synuclein nitration in synucleinopathy lesions. Science *290*, 985–989.

Giasson, B.I., Jakes, R., Goedert, M., Duda, J.E., Leight, S., Trojanowski, J.Q., and Lee, V.M.-Y. (2000b). A panel of epitope-specific antibodies detects protein domains distributed throughout human α-synuclein in Lewy bodies of Parkinson's disease. J. Neurosci. Res. *59*, 528–533.

Giasson, B.I., Duda, J.E., Forman, M.S., Lee, V.M.-Y., and Trojanowski, J.Q. (2001). Prominent perikaryal expression of α- and β-synuclein in neurons of dorsal root ganglion and in medullary neurons. Exp. Neurol. *172*, 354–362.

Golbe, L.I. (1999). α-synuclein and Parkinson's disease. Mov. Disord. *14*, 6–9.

Golbe, L.I., Di Iorio, G., Sanges, G., Lazzarini, A.M., La Sala, S., Bonavita, V., and Duvoisin, R.C. (1996). Clinical genetic analysis of Parkinson's disease in the Contursi kindred. Ann. Neurol. *40*, 767–775.

Hsu, L.J., Mallory, M., Xia, Y., Vienbergs, I., Hashimoto, M., Yoshimoto, M., Thal., L.J., Saitoh, T., and Masliah, E. (1998). Expression patterns of synuclein (non-β component of Alzheimer's disease amyloid precursor protein/α-synuclein) during murine brain development. J. Neurochem. *71*, 338–344.

Hurtig, H.I., Trojanowski, J.Q., Galvin, J., Ewbank, D., Schmidt, M.L., Lee, V.M.-Y., Clark, C.M., Glosser, G., Stern, M.B., Gollomp, S.M., and Arnold, S.E. (2000). α-synuclein cortical Lewy bodies correlate with dementia in Parkinson's disease. Neurology *54*, 1916–1921.

Ishihara, T., Hong, M., Zhang, B., Nakagawa, Y., Lee, M.K., Trojanowski, J.Q., and Lee, V.M.-Y. (1999). Age-dependent emergence and progression of a tauopathy in transgenic mice overexpressing the shortest human tau isoform. Neuron *24*, 751–762.

Jakes, R., Spillantini, M.G., and Goedert, M. (1994). Identification of two distinct synucleins from human brain. FEBS Lett. *345*, 27–32.

Julien, J.P., and Mushynski, W.E. (1998). Neurofilaments in health and disease. Prog. Nucleic Acid Res. Mol. Biol. *61*, 1–23.

Kahle, P.J., Neumann, M., Ozmen, L., Muller, V., Jacobsen, H., Schindzielorz, A., Okochi, M., Leimer, U., van der, P.H., Probst, A., et al. (2000). Subcellular localization of wild-type and Parkinson's disease-associated mutant α-synuclein in human and transgenic mouse brain. J. Neurosci. *20*, 6365–6373.

Lee, M.K., and Cleveland, D.W. (1996). Neuronal intermediate filaments. Annu. Rev. Neurosci. *19*, 187–217.

Lee, M.K., Marszalek, J.R., and Cleveland, D.W. (1994). A mutant neurofilament subunit causes massive, selective motor neuron death: implications for the pathogenesis of human motor neuron disease. Neuron *13*, 975–988.

Love, S., and Nicoll, J.A. (1992). Comparison of modified Bielschowsky silver impregnation and anti- ubiquitin immunostaining of cortical and nigral Lewy bodies. Neuropathol. Appl. Neurobiol. *18*, 585–592.

Masliah, E., Rockenstein, E., Veinbergs, I., Mallory, M., Hashimoto, M., Takeda, A., Sagara, Y., Sisk, A., and Mucke, L. (2000). Dopamin-

ergic loss and inclusion body formation in α-synuclein mice: implications for neurodegenerative disorders. Science *287*, 1265–1269.

Masliah, E., Rockenstein, E., Veinbergs, I., Sagara, Y., Mallory, M., Hashimoto, M., and Mucke, L. (2001). β-amyloid peptides enhance α-synuclein accumulation and neuronal deficits in a transgenic mouse model linking Alzheimer's disease and Parkinson's disease. Proc. Natl. Acad. Sci. USA *98*, 12245–12250.

Matsuoka, Y., Vila, M., Lincoln, S., McCormack, A., Picciano, M., LaFrancois, J., Yu, X., Dickson, D., Langston, W.J., McGowan, E., et al. (2001). Lack of nigral pathology in transgenic mice expressing human α-synuclein driven by the tyrosine hydroxylase promoter. Neurobiol. Dis. *8*, 535–539.

Mattila, P.M., Rinne, J.O., Helenius, H., Dickson, D.W., and Roytta, M. (2000). α-synuclein-immunoreactive cortical Lewy bodies are associated with cognitive impairment in Parkinson's disease. Acta Neuropathol. (Berl.) *100*, 285–290.

McKeith, I.G., Galasko, D., Kosaka, K., Perry, E.K., Dickson, D.W., Hansen, L.A., Salmon, D.P., Lowe, J., Mirra, S.S., Byrne, E.J., et al. (1996). Consensus guidelines for the clinical and pathologic diagnosis of dementia with Lewy bodies (DLB): report of the consortium on DLB international workshop. Neurology *47*, 1113–1124.

Murphy, D.D., Rueter, S.M., Trojanowski, J.Q., and Lee, V.M.-Y. (2000). Synucleins are developmentally expressed, and α-synuclein regulates the size of the presynaptic vesicular pool in primary hippocampal neurons. J. Neurosci. *20*, 3214–3220.

Paxinou, E., Chen, Q., Weisse, M., Giasson, B.I., Norris, E.H., Rueter, S.M., Trojanowski, J.Q., Lee, V.M.-Y., and Ischiropoulos, H. (2001). Induction of α-synuclein aggregation by intracellular nitrative insult. J. Neurosci. *21*, 8053–8061.

Polymeropoulos, M.H., Lavedan, C., Leroy, E., Ide, S.E., Dehejia, A., Dutra, A., Pike, B., Root, H., Rubenstein, J., Boyer, R., et al. (1997). Mutation in the α-synuclein gene identified in families with Parkinson's disease. Science *276*, 2045–2047.

Rodriguez, E.M., Yulis, R., Peruzzo, B., Alvial, G., and Andrade, R. (1984). Standardization of various applications of methacrylate embedding and silver methenamine for light and electron microscopy immunocytochemistry. Histochemistry *81*, 253–263.

Schenk, D., Barbour, R., Dunn, W., Gordon, G., Grajeda, H., Guido, T., Hu, K., Huang, J., Johnson-Wood, K., Khan, K., et al. (1999). Immunization with amyloid-β attenuates Alzheimer-disease-like pathology in the PDAPP mouse. Nature *400*, 173–177.

Schmidt, M.L., Murray, J., Lee, V.M.-Y., Hill, W.D., Wertkin, A., and Trojanowski, J.Q. (1991). Epitope map of neurofilament protein domains in cortical and peripheral nervous system Lewy bodies. Am. J. Pathol. *139*, 53–65.

Shoji, M., Harigaya, Y., Sasaki, A., Ueda, K., Ishiguro, K., Matsubara, E., Watanabe, M., Ikeda, M., Kanai, M., Tomidokoro, Y., et al. (2000). Accumulation of NACP/α-synuclein in Lewy body disease and multiple system atrophy. J. Neurol. Neurosurg. Psychiatry *68*, 605–608.

Simuni, T., and Hurtig, H.I. (2000). Parkinson's disease: the clinical picture. In Neurodegenerative Dementias, C. M. Clark and J. Q. Trojanoswki, eds. (New York: McGraw-Hill), pp. 193–203.

Spillantini, M.G., Schmidt, M.L., Lee, V.M.-Y., Trojanowski, J.Q., Jakes, R., and Goedert, M. (1997). α-synuclein in Lewy bodies. Nature *388*, 839–840.

Spillantini, M.G., Crowther, R.A., Jakes, R., Hasegawa, M., and Goedert, M. (1998). α-Synuclein in filamentous inclusions of Lewy bodies from Parkinson's disease and dementia with Lewy bodies. Proc. Natl. Acad. Sci. USA *95*, 6469–6473.

Spira, P.J., Sharpe, D.M., Halliday, G., Cavanagh, J., and Nicholson, G.A. (2001). Clinical and pathological features of a Parkinsonian syndrome in a family with an Ala53Thr α-synuclein mutation. Ann. Neurol. *49*, 313–319.

Trojanowski, J., Schuck, T., Schmidt, L.S., and Lee, V.M.-Y. (1989). Distribution of tau protein in the normal human central and peripheral nervous system. J. Histochem. Cytochem. *37*, 209–215.

Tu, P.H., Galvin, J.E., Baba, M., Giasson, B., Tomita, T., Leight, S., Nakajo, S., Iwatsubo, T., Trojanowski, J.Q., and Lee, V.M.-Y. (1998). Glial cytoplasmic inclusions in white matter oligodendrocytes of multiple system atrophy brains contain insoluble α-synuclein. Ann. Neurol. *44*, 415–422.

van der Putten, H., Wiederhold, K.H., Probst, A., Barbieri, S., Mistl, C., Danner, S., Kauffmann, S., Hofele, K., Spooren, W.P., Ruegg, M.A., et al. (2000). Neuropathology in mice expressing human α-synuclein. J. Neurosci. *20*, 6021–6029.

Wood, S.J., Wypych, J., Steavenson, S., Louis, J.C., Citron, M., and Biere, A.L. (1999). α-synuclein fibrillogenesis is nucleation-dependent. Implications for the pathogenesis of Parkinson's disease. J. Biol. Chem. *274*, 19509–19512.

Yamamoto, A., Lucas, J.J., and Hen, R. (2000). Reversal of neuropathology and motor dysfunction in a conditional model of Huntington's disease. Cell *101*, 57–66.